OXFORD

ORIGINAL ARTICLE

Eicosapentaenoic acid attenuates obesity-related hepatocellular carcinogenesis

Akane Inoue-Yamauchi[1,*], Hiroko Itagaki[1,2] and Hideaki Oda[1]

[1]Department of Pathology and [2]Department of Surgical Pathology, Tokyo Women's Medical University, Tokyo 162-0054, Japan

*To whom correspondence should be addressed. Tel: +81 3 5269 7410; Fax: +81 3 5269 7473; Email: yamauchi.akane@twmu.ac.jp

Abstract

Non-alcoholic fatty liver disease (NAFLD), the hepatic manifestation of obesity, is an emerging risk factor for hepatocellular carcinoma (HCC). Accumulating evidence has shown that chronic inflammation represents a plausible link between obesity and HCC and that the pro-inflammatory cytokine interleukin (IL)-6 contributes to the development of obesity-related HCC. In the present study, we aimed to examine the therapeutic potential of the omega-3 polyunsaturated fatty acid, eicosapentaenoic acid (EPA), which exerts anti-inflammatory effects. The results showed that the development of carcinogen-induced HCC was significantly less in mice fed a high-fat diet (HFD) supplemented with EPA than in those fed HFD only, suggesting that EPA attenuates the development of obesity-related HCC. Although EPA did not appear to affect obesity-linked inflammation, it suppressed the activation of the pro-tumorigenic IL-6 effector STAT3, contributing to the inhibition of tumor growth. These findings suggest a clinical implication of EPA as a treatment for obesity-related HCC.

Introduction

The prevalence of obesity has been steadily increasing worldwide in recent decades, with one-third of adults being classified as obese. The excess accumulation of body fat due to weight gain has a negative impact on health, and obesity has been identified as a major risk factor for type II diabetes and cardiovascular disease. Furthermore, the risk and mortality of several cancers are associated with obesity (1,2). A recent epidemiological study demonstrated that the reversal of excess weight reduced the risk of most cancers (3), suggesting that weight loss is a therapeutic approach for lowering the risk of cancer and improving the outcomes of obese patients with cancer. However, there is currently no effective treatment that enables long-term weight loss in obese adults.

HCC, a common type of liver cancer, is the third leading cause of cancer death worldwide (4). Among various cancers, HCC is the most strongly associated with obesity (1,5). HCC predominantly develops in patients with chronic inflammatory liver disease mediated by chronic viral infections and alcoholic abuse. NAFLD has recently emerged as a risk factor for HCC (6–8). NAFLD is the hepatic manifestation of obesity and includes simple steatosis, non-alcoholic steatohepatitis (NASH) and cirrhosis. Due to increases in the prevalence of obesity, NAFLD may

replace virus- and alcohol-related liver disease as the leading factor in the pathogenesis of HCC. Therefore, the development of therapeutic approaches for HCC associated with obesity-related NAFLD is needed.

The molecular link between obesity and HCC development has been extensively investigated (2,9,10). A previous study demonstrated that the pro-inflammatory cytokine IL-6 plays a role in accelerating the development of obesity-related HCC (11). These findings suggest that the disruption of IL-6-mediated inflammation is a therapeutic strategy for obesity-related HCC. EPA, an omega-3 polyunsaturated fatty acid, is a bioactive nutrient that is rich in fish oil; it has a wide range of physiological roles including anti-lipogenic and anti-inflammatory effects (12,13). These effects may be linked to clinical benefits such as the amelioration of NAFLD (14–18). On the other hand, the therapeutic efficacy of EPA for HCC, which is associated with obesity-linked inflammation, currently remains unknown.

In an attempt to assess the therapeutic potential of EPA for obesity-related HCC, we used the hepatic procarcinogen diethylnitrosamine (DEN) to induce HCC in a dietary obesity model (11). Since an HFD causes obesity and significantly enhances the development of HCC in DEN-injected mice, it is useful for

Abbreviations

DEN	diethylnitrosamine
EPA	eicosapentaenoic acid
ERK	extracellular signal-regulated kinase
HCC	hepatocellular carcinoma
HFD	high-fat diet
IL	Interleukin
JNK	c-jun N-terminal kinase
NAFLD	non-alcoholic fatty liver disease
ORO	Oil Red O
PCNA	proliferating cell nuclear antigen
SD	standard diet
STAT3	signal transducer and activator of transcription 3
TNFα	tumor necrosis factor α
TUNEL	Terminal Deoxynucleotidyl Transferase-Mediated dUTP Nick End Labeling

assessing obesity-related tumor development (11). Using this model, we herein examined the effects of EPA on the development of obesity-related HCC by feeding mice highly purified EPA. The results suggested that EPA attenuates the development of obesity-related HCC by inhibiting tumor growth, not inflammation.

Materials and methods

Materials

EPA ethyl ester (>99% purity) was obtained from Mochida Pharmaceutical (Tokyo, Japan). DEN was purchased from TCI (Tokyo, Japan).

Animals

DEN was injected intraperitoneally at 25 mg/kg into 2-week-old C57BL/6N male mice purchased from SLC Japan (Shizuoka, Japan). After 1 week, mice were separated into three dietary groups and fed a standard diet (SD) (MF; Oriental Yeast, Tokyo, Japan), HFD (HFD-60; Oriental Yeast), or HFD supplemented with 5% (wt/wt) EPA (HFD + EPA) until they were sacrificed at 9 months old. Dietary composition of the SD and HFD is shown in Supplementary Table, available at *Carcinogenesis* Online. The dietary compositions of SD and HFD were as follows: SD composed of 12.8% fat, 25.7% protein and 61.6% carbohydrates based on the caloric content and HFD composed of 62.2% fat, 18.2% protein and 19.6% carbohydrates.

Blood analysis

Plasma concentrations of aspartate aminotransferase and alanine aminotransferase were measured using a SPOTCHEM SP-4420 biochemistry analyzer (Arkray, Kyoto, Japan). Plasma concentrations of IL-6 and tumor necrosis factor α (TNFα) were determined using Quantikine ELISA kits (R&D Systems, Minneapolis, MN).

Hepatic lipid content

Triglyceride and total cholesterol contents in the liver were measured at Skylight Biotech (Akita, Japan) by the Folch technique using the Cholestest TG and Cholestest CHO kits (Sekisui Medical, Tokyo, Japan), respectively.

Histological analysis

Liver tissues were fixed in 20% formalin neutral buffer. Paraffin-embedded samples were sectioned, rehydrated and subjected to hematoxylin and eosin staining or immunohistochemistry. In immunohistochemistry, sections were blotted with an antibody specific to Ki67 (Dako, Glostrup, Denmark) or Mac-2 (CEDARLINE, Burlington, NC). Ki67-positive cells and Mac-2-positive cells were counted using e-count software (E-Path, Kanagawa, Japan) and ImageJ software (v. 1.49), respectively. Apoptosis was assessed using a Terminal Deoxynucleotidyl Transferase-Mediated dUTP Nick End Labeling (TUNEL) assay with the TACS2 TdT *in situ* Apoptosis Detection Kit (Trevigen, Gaithersburg, MD). Slides were counterstained with methyl green. Cryosections were stained with Oil Red O (ORO) to evaluate hepatic deposits.
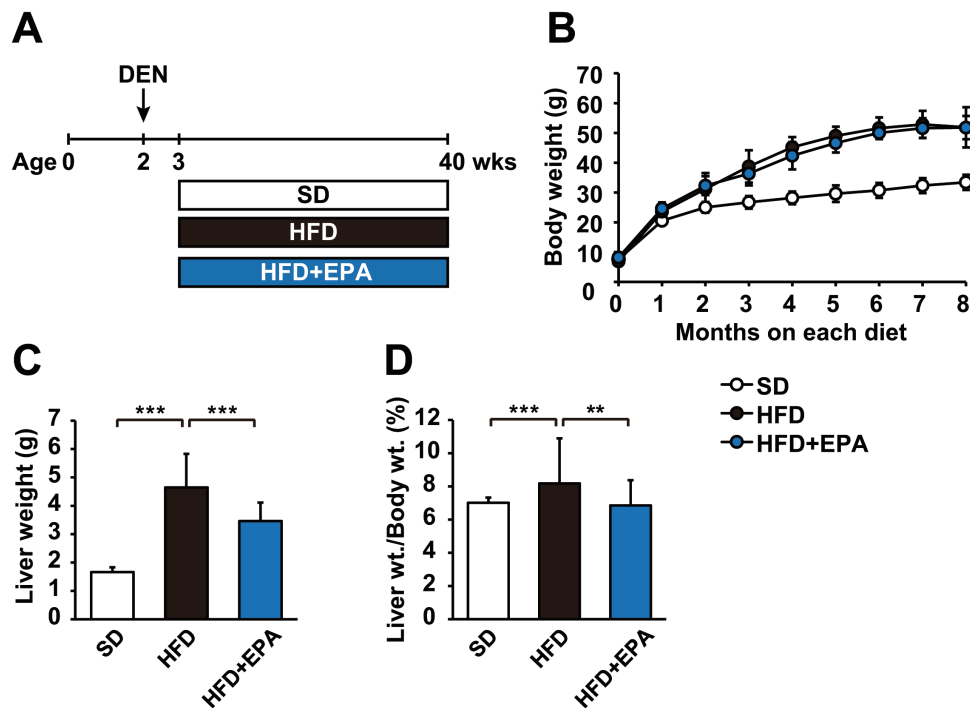
Figure 1. EPA has no effect on HFD-induced obesity. (**A**) Experimental protocol of the EPA treatment for the obesity-related HCC mouse model. (**B**) Growth curve of DEN-injected mice fed SD, HFD or HFD + EPA. Liver weight (**C**) and the ratio of liver weight to body weight of mice (**D**) from three dietary groups at 9 months old. All values represent the mean ± SD (*n* = 10–12). **P < 0.01; ***P < 0.001.

Reverse transcription and quantitative PCR

Total RNA was extracted from liver tissues using an RNA purification kit (Qiagen, Hilden, Germany) according to the manufacturer's instructions. Reverse transcription was performed with oligo-dT plus random decamer primers (Thermo Fisher Scientific, Waltham, MA) with SuperScript II (Thermo Fisher Scientific). Quantitative PCR was performed with SYBR Green Master Mix (Applied Biosystems, Foster City, CA) in duplicate with the indicated gene-specific primers. Quantitative PCR was performed on a StepOne plus (Applied Biosystems). Data were analyzed by normalization against 18s. The primers used for quantitative reverse transcription PCR are listed below: *Tnf*, 5′-CGA GGA CAG CAA GGG ACT AGC-3′ and 5′-CCT CTT CTG CCA GTT CCA CGT C-3′; *Il-6*, 5′-GAG ACT TCC ATC CAG TTG CCT TCT TG-3′ and 5′-TCT GCA AGT GCA TCA TCG TTG TTC-3′; *Adgre1*, 5′-TAT GCC ACC TGC ACT GAC ACC-3′ and 5′-AGA CAG CTG CAC TTG CT CTC-3′; *Ly6g*, 5′-CCA CCT GAG ACT TCC TGC AAC AC-3′ and 5′-AAC TGC TGC ATT GCA GAG GTC TTC-3′.

Antibodies and immunoblot analysis

Tissues were lysed in RIPA buffer [10 mM sodium phosphate (pH 7.2), 150 mM NaCl, 1% Nonidet P-40, 1% sodium deoxycholate, 0.1% sodium dodecyl sulfate, 2 mM ethylenediaminetetraacetic acid, 50 mM NaF and 0.2 mM Na_3VO_4]. Protein concentrations were measured using a BCA kit (Thermo Fisher Scientific). Sixty microgram of protein were separated by sodium dodecyl sulfate–polyacrylamide gel electrophoresis on 10% gels and transferred to polyvinylidene difluoride membranes (Immobilon-P, Millipore, Bedford, MA). Antibody detection was accomplished using an enhanced chemiluminescence method (ECL Western Blotting Substrate,

Thermo Fisher Scientific) and LAS-500 Imaging system (FUJIFILM, Tokyo, Japan). The antibodies used for the immunoblot analysis were as follows: anti-PCNA (PC10) (Dako, Glostrup, Denmark), anti-γ-tubulin (T6557) (Sigma–Aldrich, St. Louis, MO), anti-phospho-STAT3 (D3A7), anti-phospho-ERK, anti-phospho-JNK (81E11), anti-STAT3 (D3Z2G), anti-ERK (137F5) and anti-JNK (56G8) (Cell Signaling Technology, Danvers, MA). The relative signal intensity of each protein was measured with ImageJ software (v. 1.49). Densitometric measurements were expressed as arbitrary units of the phosphorylation levels for extracellular signal-regulated kinase (ERK), c-jun N-terminal kinase (JNK) and signal transducer and activator of transcription 3 (STAT3) and were normalized to the total amount of each protein. The relative signal intensity of proliferating cell nuclear antigen (PCNA) was normalized to γ-tubulin.

Statistical analysis

Data are presented as mean ± standard deviation (SD), and $P < 0.05$ was considered to be significant. Statistical analyses were performed using analysis of variance followed by Tukey's test. Differences between two groups were compared using Student's *t*-test.

Results

EPA inhibits hepatic steatosis in obese mice

To assess the effects of EPA on the development of obesity-related HCC, we used a DEN-induced HCC mouse model fed HFD consisting of 62.2 kcal% fat ([11]). DEN-injected C57BL/6N male
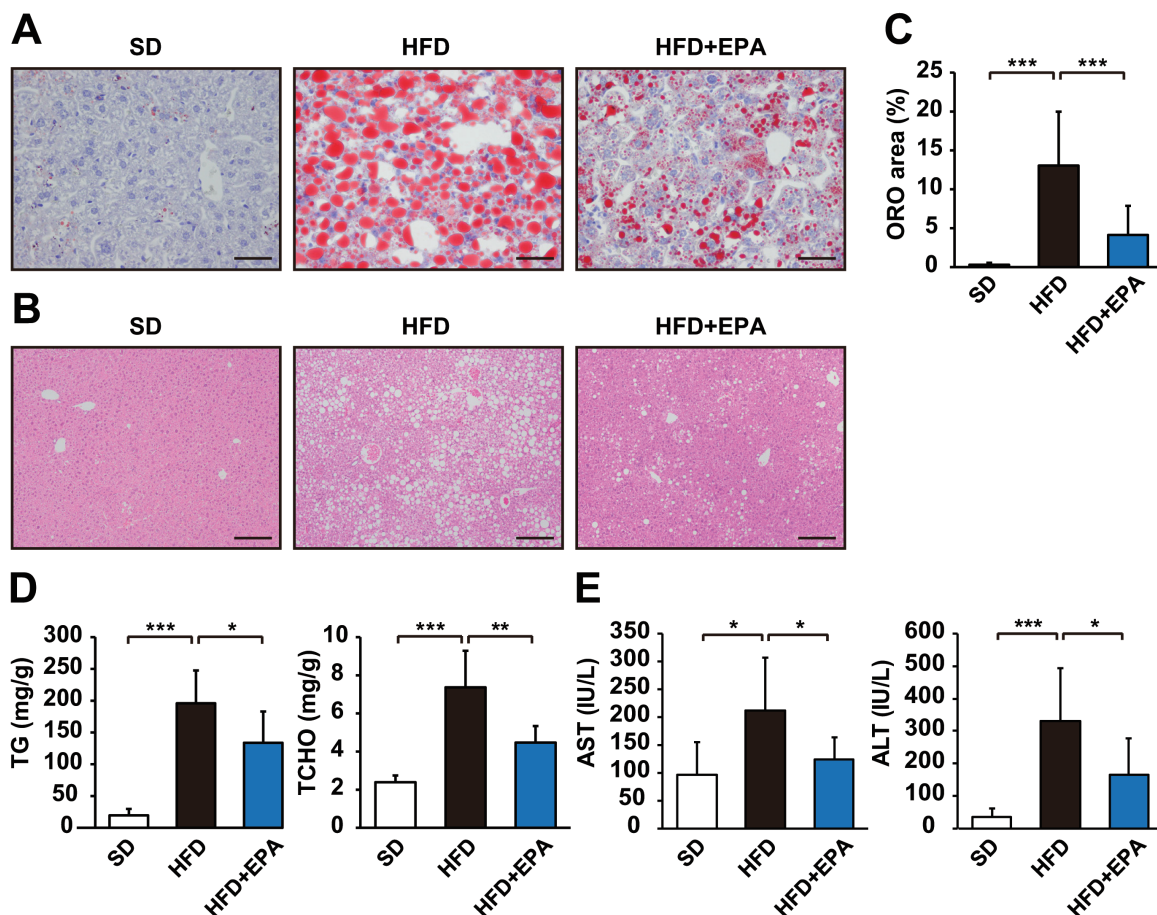
Figure 2. EPA ameliorates hepatic steatosis in obese mice. ORO staining (**A**) and hematoxylin and eosin (HE) staining (**B**) of liver sections from DEN-injected mice fed SD, HFD or HFD + EPA for 37 weeks. (**C**) Percentage of the area occupied by ORO staining in each field ($n = 3–4$). (**D**) Liver triglyceride (TG) and total cholesterol (TCHO) levels in DEN-injected mice in each dietary group were measured at 9 months old ($n = 6–8$). (**E**) Plasma concentrations of aspartate aminotransferase (AST) and alanine aminotransferase (ALT) in DEN-injected mice in each dietary group were measured at 9 months old ($n = 9–12$). Scale bars = 50 μm (**A**) and 200 μm (**B**). All values represent the mean ± SD. *$P < 0.05$; **$P < 0.01$; ***$P < 0.001$.
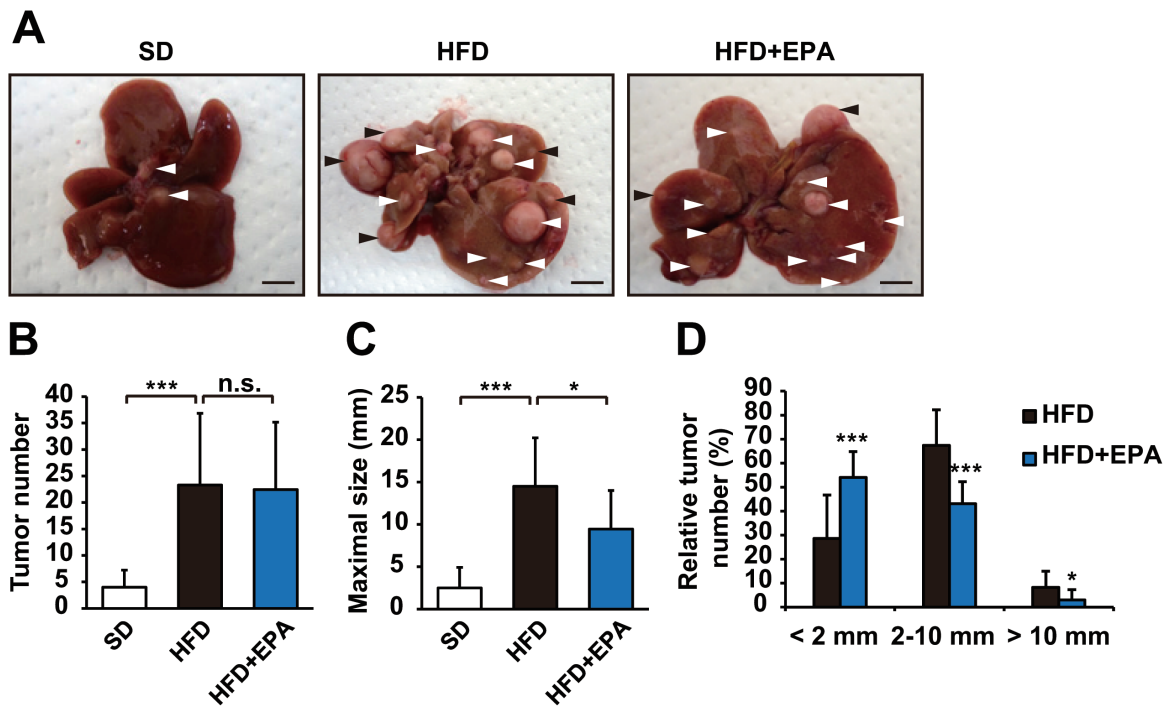
Figure 3. EPA attenuates obesity-enhanced hepatocarcinogenesis. Gross liver morphology (**A**), tumor numbers (**B**), tumor maximal sizes (**C**) and tumor size distribution (**D**) from DEN-injected mice fed SD, HFD or HFD + EPA for 37 weeks. Arrows indicate tumors (**A**). Scale bars = 10 mm. All values represent the mean ± SD (*n* = 10–12). *P < 0.05; ***P < 0.001. n.s. indicates not significant.

mice were separated into three dietary groups and fed SD, HFD or HFD + EPA until 9 months old (Figure 1A). As expected, HFD-fed mice exhibited more accelerated weight gain and higher liver weights than SD-fed control mice (Figure 1B and C). EPA had no obvious effect on HFD-induced weight gain (Figure 1B), but reduced increased liver weight (Figure 1C), resulting in a lower ratio of liver weight to body weight than that of HFD-fed mice (Figure 1D). A histological analysis using ORO staining and Hematoxylin and eosin staining showed that EPA significantly decreased hepatic lipid accumulation in HFD-fed mice (Figure 2A, B and C). The elevated hepatic triglyceride and total cholesterol levels in HFD-fed mice were reduced in HFD + EPA-fed mice (Figure 2D). Additionally, EPA reduced elevated plasma levels of aspartate aminotransferase and alanine aminotransferase, markers of hepatic injury, in HFD-fed mice (Figure 2E). These results indicate that EPA ameliorates fatty liver without affecting obesity.

EPA attenuates obesity-related HCC development

DEN is a procarcinogen that is widely used to induce HCC in mice. We found that HFD markedly enhanced the development of HCC in a DEN-induced HCC model, as previously reported (11); tumor formation assessed by number and size was significantly greater in HFD-fed mice than in SD-fed mice (Figure 3A, B and C). HFD + EPA-fed mice developed a similar number of tumors to HFD-fed mice (Figure 3B). In contrast, HFD + EPA-fed mice had a larger number of smaller tumors than HFD-fed mice (Figure 3D) and the maximal tumor size that developed in HFD + EPA-fed mice was significantly decreased (Figure 3C). These results suggest that EPA affects tumor growth more than tumor initiation.
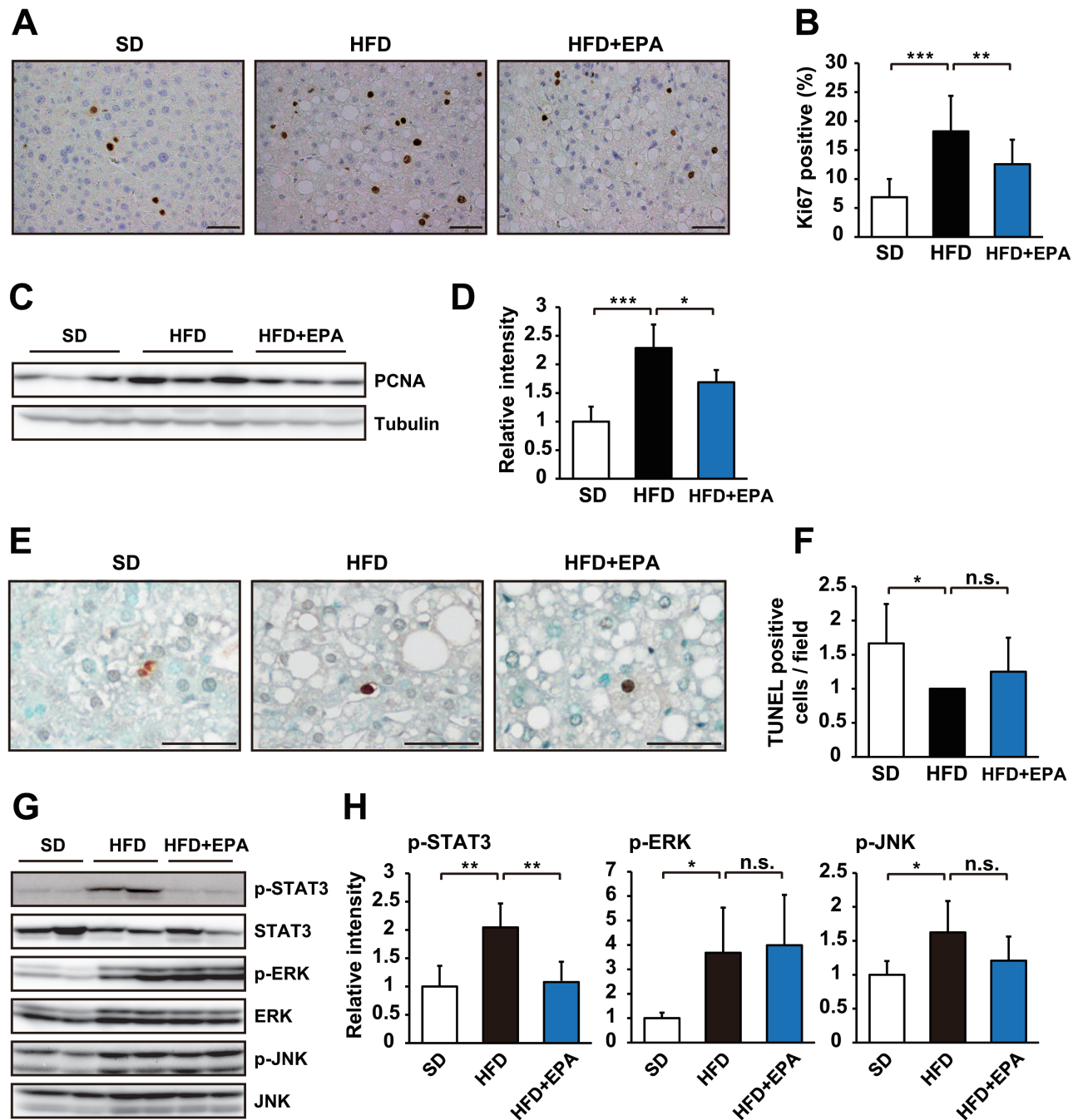
EPA inhibits obesity-enhanced STAT3 activation and tumor cell proliferation

Since the balance between proliferation and apoptosis regulates tumor growth, we examined these cellular responses in tumors

from HFD-fed mice and HFD + EPA-fed mice. The staining of a cell proliferation marker Ki67 showed that EPA significantly inhibited increases in tumor cell proliferation in HFD-fed mice (Figure 4A and B). Similar results were obtained by an immunoblot analysis using another proliferation marker PCNA (Figure 4C and D). In contrast, EPA had no effect on apoptosis in tumors, which was assessed by TUNEL staining (Figure 4E and F). These results indicate that EPA influences tumor cell proliferation not apoptosis. To elucidate the molecular basis underlying the anti-proliferative effects of EPA on HFD-promoted tumor development, we examined the activation of the oncogenic mediators, STAT3, ERK and JNK, which regulate the development of HCC (11). The phosphorylation of these proteins in tumor tissue from HFD- or HFD + EPA-fed mice was evaluated as a measure of their activation status. As reported previously (11), these signals were elevated in HFD-fed mice (Figure 4G and H). We found that EPA significantly inhibited the HFD-induced activation of STAT3 (Figure 4G and H), but not ERK or JNK (Figure 4G and H). These results suggest that EPA affects tumor growth through its anti-proliferative effect by suppressing the activation of STAT3.

EPA has no obvious effect on inflammatory responses caused by obesity

Since EPA is known to exhibit anti-inflammatory activity (12,13,19), we hypothesized that it inhibits HFD-enhanced tumor development by suppressing the inflammatory responses involved in the development of obesity-related HCC. Therefore, we examined macrophage infiltration in the liver by immunohistochemistry with Mac-2-specific antibodies. The results revealed that enhanced hepatic infiltration by Mac-2-positive macrophages in HFD-fed mice was not affected by EPA (Figure 5A and B). Macrophage infiltration was similar between HFD + EPA-fed mice and HFD-fed mice (Figure 5A and B). We also compared the gene expression of TNFα, IL-6, F4/80 and Gr-1, markers of inflammation, in livers

Figure 4. EPA affects obesity-enhanced STAT3 activation and tumor cell proliferation. (**A**) Ki67 immunostaining of tumor areas in livers from DEN-injected mice fed SD, HFD or HFD + EPA for 37 weeks. (**B**) The percentage of Ki67-positive cells per field (*n* = 7). (**C**) Tumor liver tissues from DEN-injected mice in each of the three dietary groups were analyzed by immunoblotting with the indicated antibodies. (**D**) Ratio of PCNA expression to γ-tubulin (*n* = 5). (**E**) TUNEL staining of tumor areas in livers from DEN-injected mice fed SD, HFD or HFD + EPA for 37 weeks. (**F**) The number of TUNEL-positive cells per field (*n* = 3). (**G**) Tumor liver tissues from DEN-injected mice in each of the three dietary groups were analyzed by immunoblotting with the indicated antibodies. (**H**) Ratio of tyrosine phosphorylation of STAT3, ERK and JNK to the total amount of each protein (*n* = 3–7). The mean relative intensity of the phosphorylation of each protein in SD mice was arbitrarily defined as 1. Scale bars = 50 µm. All values represent the mean ± SD. *$P < 0.05$; **$P < 0.01$; ***$P < 0.001$. n.s. indicates not significant.

from HFD-fed mice and HFD + EPA-fed mice. Consistent with Mac-2 staining results, a qRT-PCR showed that EPA did not exert any significant effects on HFD-induced inflammatory responses; therefore, the expression levels of these inflammatory markers were similar in HFD + EPA-fed mice and HFD-fed mice (Figure 5C). EPA also exhibited no significant effect on the level of circulating IL-6 and TNFα in HFD-fed mice

(Figure 5D). These results indicate that EPA does not appear to affect HFD-induced inflammation.

Discussion

By using a carcinogen-injected dietary obesity model, we herein showed that EPA attenuated the development of HCC associated
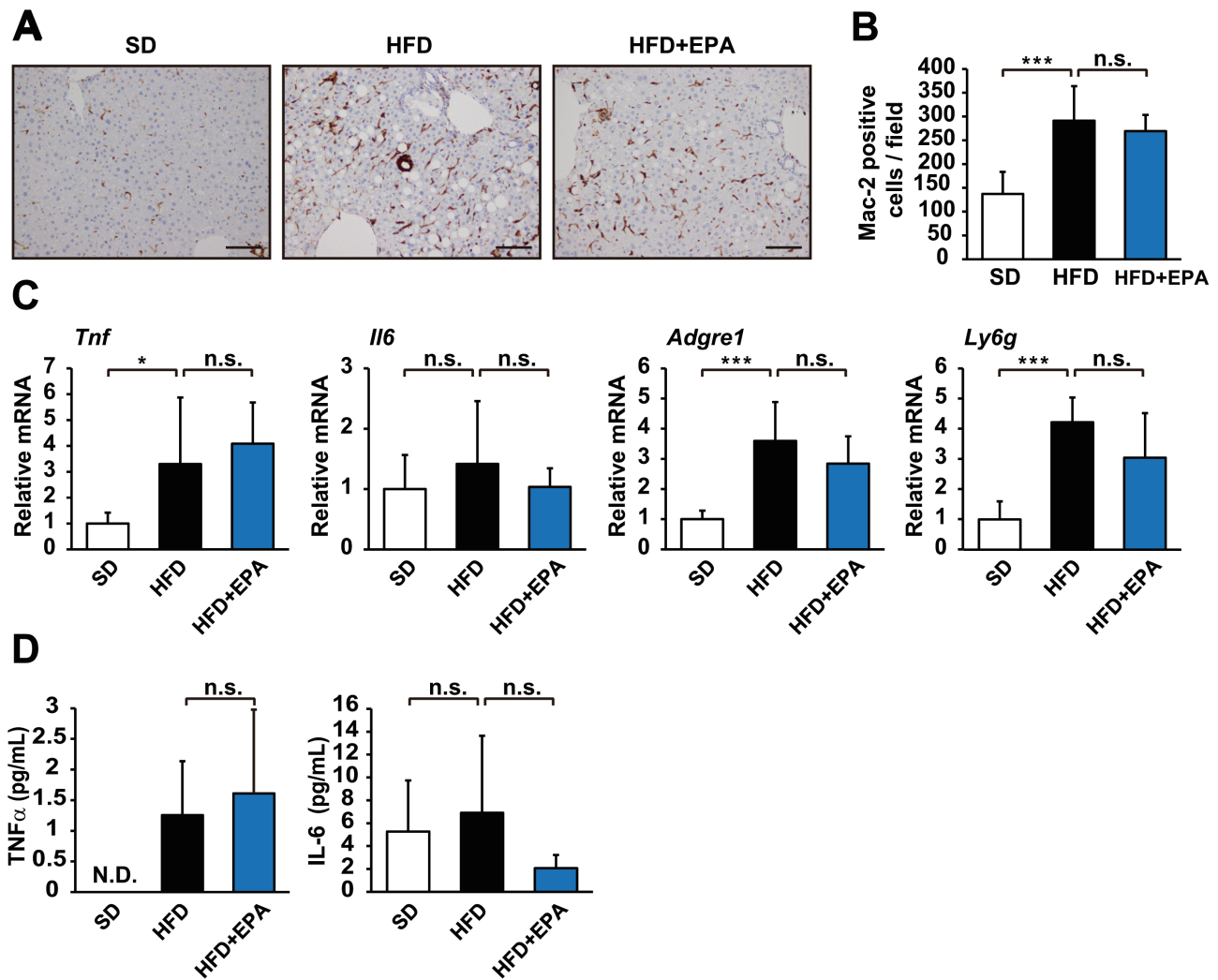
Figure 5. EPA does not affect obesity-linked hepatic inflammation. (**A**) Mac-2 immunostaining of livers from DEN-injected mice fed SD, HFD or HFD + EPA for 37 weeks. (**B**) The number of Mac-2-positive cells per field (*n* = 6). (**C**) mRNA levels of inflammatory markers in livers from each dietary group were assessed by qRT-PCR (*n* = 6–8). The mean relative amount of each mRNA in SD mice was arbitrarily defined as 1. (**D**) The concentrations of IL-6 and TNFα in the plasma of mice from each dietary group were assessed by enzyme-linked immunosorbent assay (*n* = 7–10). N.D. indicates not detected. Scale bars = 100 μm. All values represent the mean ± SD. *P < 0.05; ***P < 0.001. n.s. indicates not significant.

with obesity. Interestingly, we found that EPA inhibited obesity-induced STAT3 activation and tumor cell proliferation not hepatic inflammation.

Although the anti-inflammatory effects of EPA are well known (12,13,19), it had no obvious effect on inflammatory responses in the tumor-bearing dietary obesity model, as assessed by macrophage infiltration and the expression of inflammatory markers. In support of our results, a previous study reported that hepatic inflammation in Western diet-fed MCR4-deficient mice was not inhibited by EPA (17). These findings suggest that the anti-inflammatory effects of EPA depend on the pathogenesis of inflammation. Additionally, the anti-inflammatory effect of EPA may depend on the strength of the inflammation. Indeed, it has been reported that the EPA had no inhibitory effect on low levels of inflammation in THP-1 macrophages (20). The level of inflammation in HFD-fed mice may not be enough to elicit the anti-inflammatory effect of EPA.

IL-6 contributes to obesity-linked tumor-promoting inflammation (9,10). Obesity appears to stimulate inflammation through oxidative stress caused by excessive amounts of toxic lipids including free fatty acids and free cholesterol (21), resulting in the activation of Kupffer cells. Activated Kupffer cells produce IL-6 in order to recruit inflammatory cells, thereby propagating inflammatory responses (22,23). Besides its role as an effector cytokine of inflammation, IL-6 acts as a tumor-promoting cytokine (23,24). STAT3 is a potent effector of pro-tumorigenic IL-6 signaling and regulates genes that mediate cancer cell proliferation. The aberrant activation of STAT3 is frequently associated with various cancers including HCC (25,26). Thus, the blockade of STAT3 signaling may ameliorate cancer associated with chronic inflammation. We herein demonstrated that EPA inhibited the activation of STAT3, which suppressed tumor cell proliferation. Since EPA has been reported to inhibit IL-6-induced STAT3 activation and proliferation of hepatoma HepG2 cells (27,28), it may directly act on liver tumor cells in obese mice in order to inhibit the activation of STAT3 and proliferation. Based on the similar level of IL-6 in HFD + EPA-fed mice and HFD-fed mice, the target of EPA for the inhibition of STAT3 may be downstream of the IL-6 receptor. Further studies are needed to elucidate the mechanisms underlying the inhibition of STAT3

by EPA. Nevertheless, since EPA is known to modify the membrane composition of phospholipids (12), it may inhibit the activation of STAT3 by influencing membrane lipid rafts, at which various signaling molecules gather upon stimulation, thereby facilitating signal transduction (29). In support of this hypothesis, a previous study reported that raft inhibitors abrogated the activation of STAT3 on IL-6 in myeloma cells (30).

EPA has been shown to inhibit the development of HCC in NASH-like livers from mice lacking hepatocellular PTEN (16). Although fatty liver diseases were promoted in these mice, they were not obese (31,32), indicating that HCC caused by a hepatic PTEN deficiency has a different etiology from obesity-related HCC. Since diet is a primary driver of obesity and NAFLD, we used a HFD obesity model to test the therapeutic potential of EPA for obesity-related HCC. This model imitates obesity and the NAFLD-related phenotype (33); however, inflammation and fibrosis that developed in this model were not as robust as in human patients, indicating that this model does not fully recapitulate the process of human steatosis disease. On the other hand, although the pathogenesis of HCC in NAFLD is not fully understood, a growing body of evidence indicates that HCC may develop in NAFLD patients without cirrhosis (6,8). Previous studies reported that a significant number of NAFLD-related HCCs did not develop extensive fibrosis. Furthermore, HCC has also been shown to develop in cases of fatty liver without steatohepatitis and fibrosis (6,34). Thus, the dietary obesity model used in the present study may be advantageous for analyzing these cases of NAFLD-related HCC. However, additional studies on other obesity-associated NAFLD models are needed to confirm the universality of EPA for the treatment of HCC associated with obesity independent of etiology. HFD-fed MCR4-deficient mice represent one testable model; they are obese, attain the human NASH-like phenotype, including hepatocyte ballooning and hepatic fibrosis, and ultimately develop HCC (35).

Collectively, the results of the present study show that the inhibition of pro-tumorigenic IL-6 effector STAT3 activation by EPA may contribute to the attenuation of HCC associated with obesity, indicating the potential of EPA as a new therapeutic approach for obesity-related HCC treatment.

Supplementary material

Supplementary data are available at *Carcinogenesis* online.

Acknowledgements

References

1. Calle, E.E. *et al.* (2003) Overweight, obesity, and mortality from cancer in a prospectively studied cohort of U.S. adults. N. Engl. J. Med., 348, 1625–1638.
2. Calle, E.E. *et al.* (2004) Overweight, obesity and cancer: epidemiological evidence and proposed mechanisms. Nat. Rev. Cancer, 4, 579–591.
3. Lauby-Secretan, B. *et al.*; International Agency for Research on Cancer Handbook Working Group. (2016) Body fatness and cancer – viewpoint of the IARC Working Group. N. Engl. J. Med., 375, 794–798.
4. El-Serag, H.B. *et al.* (2007) Hepatocellular carcinoma: epidemiology and molecular carcinogenesis. Gastroenterology, 132, 2557–2576.
5. Caldwell, S.H. *et al.* (2004) Obesity and hepatocellular carcinoma. Gastroenterology, 127 (5 suppl. 1), S97–S103.
6. Baffy, G. *et al.* (2012) Hepatocellular carcinoma in non-alcoholic fatty liver disease: an emerging menace. J. Hepatol., 56, 1384–1391.
7. Michelotti, G.A. *et al.* (2013) NAFLD, NASH and liver cancer. Nat. Rev. Gastroenterol. Hepatol., 10, 656–665.
8. Marengo, A. *et al.* (2016) Liver cancer: connections with obesity, fatty liver, and cirrhosis. Annu. Rev. Med., 67, 103–117.
9. Renehan, A.G. *et al.* (2015) Adiposity and cancer risk: new mechanistic insights from epidemiology. Nat. Rev. Cancer, 15, 484–498.
10. Park, J. *et al.* (2014) Obesity and cancer – mechanisms underlying tumour progression and recurrence. Nat. Rev. Endocrinol., 10, 455–465.
11. Park, E.J. *et al.* (2010) Dietary and genetic obesity promote liver inflammation and tumorigenesis by enhancing IL-6 and TNF expression. Cell, 140, 197–208.
12. Calder, P.C. (2012) Mechanisms of action of (n – 3) fatty acids. J. Nutr., 142, 592S–599S.
13. Calder, P.C. (2013) Omega-3 polyunsaturated fatty acids and inflammatory processes: nutrition or pharmacology? Br. J. Clin. Pharmacol., 75, 645–662.
14. Scorletti, E. *et al.* (2013) Omega-3 fatty acids, hepatic lipid metabolism, and nonalcoholic fatty liver disease. Annu. Rev. Nutr., 33, 231–248.
15. Jump, D.B. *et al.* (2015) Potential for dietary ω-3 fatty acids to prevent nonalcoholic fatty liver disease and reduce the risk of primary liver cancer. Adv. Nutr., 6, 694–702.
16. Ishii, H. *et al.* (2009) Eicosapentaenoic acid ameliorates steatohepatitis and hepatocellular carcinoma in hepatocyte-specific Pten-deficient mice. J. Hepatol., 50, 562–571.
17. Konuma, K. *et al.* (2015) Eicosapentaenoic acid ameliorates non-alcoholic steatohepatitis in a novel mouse model using melanocortin 4 receptor-deficient mice. PLoS One, 10, e0121528.
18. Suzuki-Kemuriyama, N. *et al.* (2016) Different effects of eicosapentaenoic and docosahexaenoic acids on atherogenic high-fat diet-induced non-alcoholic fatty liver disease in mice. PLoS One, 11, e0157580.
19. Hardman, W.E. (2004) (n – 3) fatty acids and cancer therapy. J. Nutr., 134 (suppl. 12), 3427S–3430S.
20. Mullen, A. *et al.* (2010) Anti-inflammatory effects of EPA and DHA are dependent upon time and dose-response elements associated with LPS stimulation in THP-1-derived macrophages. J. Nutr. Biochem., 21, 444–450.
21. Solinas, G. *et al.* (2006) Saturated fatty acids inhibit induction of insulin gene transcription by JNK-mediated phosphorylation of insulin-receptor substrates. Proc. Natl Acad. Sci. USA, 103, 16454–16459.
22. Kamimura, D. *et al.* (2003) IL-6 signal transduction and its physiological roles: the signal orchestration model. Rev. Physiol. Biochem. Pharmacol., 149, 1–38.
23. Naugler, W.E. *et al.* (2008) The wolf in sheep's clothing: the role of interleukin-6 in immunity, inflammation and cancer. Trends Mol. Med., 14, 109–119.
24. Turkson, J. *et al.* (2000) STAT proteins: novel molecular targets for cancer drug discovery. Oncogene, 19, 6613–6626.
25. Yu, H. *et al.* (2004) The STATs of cancer – new molecular targets come of age. Nat. Rev. Cancer, 4, 97–105.
26. Haura, E.B. *et al.* (2005) Mechanisms of disease: insights into the emerging role of signal transducers and activators of transcription in cancer. Nat. Clin. Pract. Oncol., 2, 315–324.
27. Wang, T.M. *et al.* (2013) Docosahexaenoic acid and eicosapentaenoic acid reduce C-reactive protein expression and STAT3 activation in IL-6-treated HepG2 cells. Mol. Cell. Biochem., 377, 97–106.
28. Lim, K. *et al.* (2009) Omega-3 polyunsaturated fatty acids inhibit hepatocellular carcinoma cell growth through blocking beta-catenin and cyclooxygenase-2. Mol. Cancer Ther., 8, 3046–3055.
29. Pike, L.J. (2003) Lipid rafts: bringing order to chaos. J. Lipid Res., 44, 655–667.
30. Zheng, X. *et al.* (2015) Different associations of CD45 isoforms with STAT3, PKC and ERK regulate IL-6-induced proliferation in myeloma. PLoS One, 10, e0119780.
31. Horie, Y. *et al.* (2004) Hepatocyte-specific Pten deficiency results in steatohepatitis and hepatocellular carcinomas. J. Clin. Invest., 113, 1774–1783.

32. Peyrou, M. *et al.* (2015) Hepatic PTEN deficiency improves muscle insulin sensitivity and decreases adiposity in mice. J. Hepatol., 62, 421–429.

33. Hebbard, L. *et al.* (2011) Animal models of nonalcoholic fatty liver disease. Nat. Rev. Gastroenterol. Hepatol., 8, 35–44.

34. Margini, C. *et al.* (2016) The story of HCC in NAFLD: from epidemiology, across pathogenesis, to prevention and treatment. Liver Int., 36, 317–324.

35. Itoh, M. *et al.* (2011) Melanocortin 4 receptor-deficient mice as a novel mouse model of nonalcoholic steatohepatitis. Am. J. Pathol., 179, 2454–2463.